

ANL/RE/CP--81947
CONF-931160--41

The submitted manuscript has been authored by a contractor of the U. S. Government under contract No. W-31-109-ENG-38. Accordingly, the U. S. Government retains a nonexclusive, royalty-free license to publish or reproduce the published form of this contribution, or allow others to do so, for U. S. Government purposes.

DIRECT CONTAINMENT HEATING EXPERIMENTS IN ZION NUCLEAR POWER PLANT GEOMETRY USING PROTOTYPIC MATERIALS

J. L. Binder, L. M. McUmbler and B. W. Spencer
Argonne National Laboratory
9700 S. Cass Avenue Argonne, IL 60439 USA
(708) 252-4758/FAX (708) 252-6080

ABSTRACT

Direct Containment Heating (DCH) experiments have been completed which utilize prototypic core materials. The experiments reported on here are a continuation of the Integral Effects Testing (IET) DCH program. The experiments incorporated a 1/40 scale model of the Zion Nuclear Power Plant containment structures. The model included representations of the primary system volume, RPV head, cavity and instrument tunnel, and the lower containment structures. The experiments were steam driven. Alumina thermite with chromium was used as a core melt simulant in the earlier IET experiments. These earlier experiments at Argonne National Laboratory (ANL) and Sandia National Laboratories (SNL) provided useful data on the effect of scale on DCH phenomena; however, a significant concern concerns the potential experiment distortions caused by the use of non-prototypic iron/alumina simulant. Therefore, further testing with prototypic materials was carried out at ANL. Three tests have been completed, DCH-U1A, U1B and U2. DCH-U1A and U1B used an inerted containment atmosphere and are similar to the IET-IRR test with iron/alumina thermite. U2 employed nominally the same atmosphere as U1A and U1B but the addition of its counterpart iron/alumina test, IET-6. All tests with prototypic material, have produced lower peak pressure rises; 45, 111 and 185 kPa in U1A, U1B and U2, compared to 150 and 250 kPa IET-IRR and IET-6. Steam production, due to metal-steam reactions, was 33% in U1B and U2 compared to IET-IRR and IET-6. The steam production efficiency was consistently lower for the corium tests compared to the IET tests.

INTRODUCTION

Risk studies of U. S. nuclear power plants have attracted attention on low probability, beyond design basis, accidents. These accidents involve a core melt, failure of the vessel lower head, failure of the lower head, and release to the containment. The release of the molten material (corium) to the containment can produce high pressure loadings that pose a threat to the integrity of the containment. Of interest here is a corium release from a PWR while the vessel is at elevated pressure. In this case the corium will be forcibly ejected into the containment cavity. An event of this type is termed a High

Pressure Melt Ejection (HPME). The fundamental question concerning a HPME is: Will the HPME cause an energy transfer to the containment atmosphere large enough to produce a pressure load that threatens the containment integrity? The transfer of energy to the containment atmosphere is termed Direct Containment Heating (DCH).

The U. S. Nuclear Regulatory Commission has been sponsoring a research program to resolve the DCH issue. An important part of this effort is an integral effects testing program. The initial objective of this program was to assess the effects of experiment scale on DCH phenomena. This was accomplished by performing integral and counterpart experiments in two different facilities. Experiments at 1/40th linear scale were conducted at Argonne National Laboratory^{1,2,3} and at 1/10th linear scale at Sandia National Laboratories.^{4,5,6} The experiments incorporate melt ejection from the vessel, high pressure blowdown of the primary system, entrainment and sweepout of debris from the cavity, transport and trapping in the lower containment subcompartments, oxidation of metallic constituents, combustion of hydrogen, and heat transfer to and vaporization of water in the containment. The experiments employed the geometry of the Zion Nuclear Power Plant (NPP). The major objective in this program was met and the effect of experiment scale was found to be small over the range of experimental conditions considered. However, a significant question remained concerning the degree of distortion introduced by the use of the non-prototypic iron/alumina thermite as a core melt simulant. The experiments reported on here addressed this issue by using prototypic materials.

EXPERIMENT DESCRIPTION

The experiments were conducted in the Corium Expansion Vessel Interaction (COREXIT) facility at Argonne National Laboratory. The facility is designed to accommodate expansion vessel severe accident experiments with prototypic materials. The major components of the facility are depicted schematically in Figure 1. Major components include an explosion resistant containment cell, a 1.51 m³ expansion vessel, and a high pressure steam delivery system. The steam delivery system consists of a high pressure steam boiler and an accumulator volume scaled to the primary system volume of the power plant. High pressure driving steam is supplied to the experiment by pressurizing the accumulator volume.

MASTER

rp

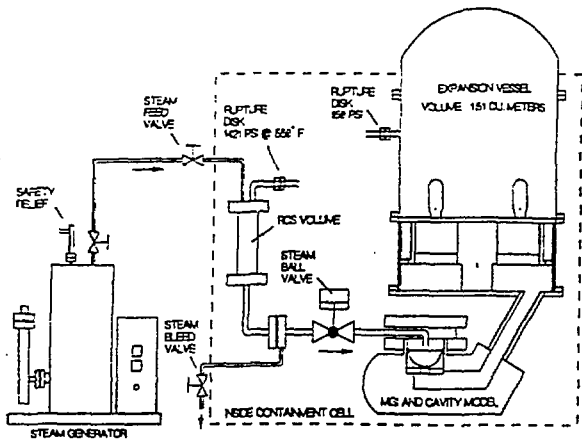


Figure 1 The COREXIT Facility

The accumulator is connected to a melt generator and injector (MGI) via piping and a fast opening ball valve. The present experimental apparatus is depicted schematically in Figures 1, 2 and 3.

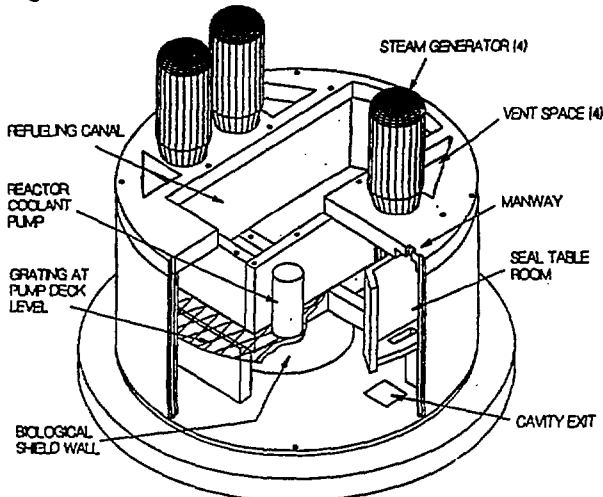


Figure 2 The 1/40 Scale Zion Subcompartment Model

The apparatus consists of nominally 1/40 scale models of the Zion Nuclear Power Plant (NPP) reactor cavity and instrument tunnel, reactor vessel bottom and a lower containment subcompartment model. The subcompartment model includes the seal table room, biological shield wall, steam generators, reactor coolant pumps, refueling canal, pump deck floor grating, and operating deck floor.

The main experiment procedures were as follows: 1) Thermite powders for generating the core melt were loaded into the melt generator and injector. The experiment apparatus was assembled. 2) The accumulator and expansion vessel were set to the specified initial conditions. 3) Data acquisition was started. The thermite powders were ignited in the MGI. 4) When the thermite reaction neared completion, steam was applied to the MGI. This is followed by the failure of a brass plug at the bottom of the MGI.

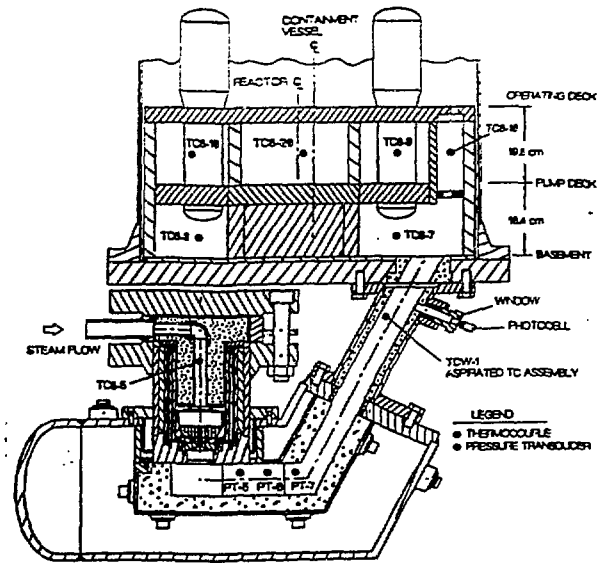


Figure 3 The 1/40 Scale Zion Cavity and Subcompartment Model initiating the HPME.

A variety of measurements are taken during the HPME sequence. These include pressure and gas temperature measurements in the accumulator, MGI, cavity, subcompartment, and expansion vessel upper dome. Gas temperatures in the cavity are measured with an aspirated Type C thermocouple. The gas composition is measured at various locations by gas sample bottles. The gas sample bottles are evacuated prior to the test and opened at predetermined times after the start of the HPME. The background gas composition is also sampled. The gas sample bottles are analyzed posttest. The ultimate disposition of the debris is measured by posttest vacuuming and weighing samples from various locations of interest.

A prototypic core melt was produced for the experiments by first mixing powders of uranium, zirconium, iron oxide (Fe_2O_3), and chromium trioxide (CrO_3). When ignited the powders react exothermically to produce a molten mixture. The amounts of each powder were selected to closely produce the anticipated composition for a core melt following a station blackout.⁷ The experiment corium composition was 57.8 mass% UO_2 , 10.5 mass% ZrO_2 , 14.3 mass% Fe, 13.7 mass% Zr, and 3.7 mass% Cr. In development tests the initial melt temperature was measured with tantalum sheathed Type C thermocouples and pyrometers to be approximately 2700 K.

The experimentally produced corium closely matches the prototypic melt in terms of composition and thermophysical properties. Comparison of the prototypic melt to the iron/alumina thermite with chromium melt, used in the earlier IET tests at ANL and SNL, reveals some significant differences. The specific enthalpy of the corium at 2700 K is 1.2 MJ/kg compared to 2.25 MJ/kg for the iron-alumina simulant at its measured initial temperature of 2500 K. The metal fraction of the corium is 32% compared to 63% for the iron alumina simulant. The oxide will have a considerably higher freezing range than the metal. Therefore,

freezing effects on the heat transfer to the containment atmosphere is expected to be more significant for the corium. Freezing of the corium will result in lower debris entrainment rates and lesser fragmentation. Although the corium has a lower enthalpy and lower metal fraction than the iron alumina thermite, the corium has a larger chemical energy content. Table 1 gives the relevant data on the oxidation of the two melt simulants with steam. The metal phases are made up of strong oxidizers (zirconium, chromium and/or aluminum) and a weak oxidizer (iron). The strong oxidizers can be expected to react readily with the steam to liberate energy and produce hydrogen. However, the iron will not readily react with the steam, on the time scale of a HPME. The impact of this on the appropriateness of the iron/alumina thermite simulant can be seen in Table 1. Whereas, the iron/alumina simulant has a large metal fraction, a majority, 81%, is iron. In contrast 45% of the corium metal phase is iron. Therefore, the corium will produce more hydrogen and liberate more chemical energy due to reactions with steam, if fully oxidized. In addition to the difference in the energy content of the melts there exists a considerable difference in the material density. The density of the corium is approximately a factor of two greater than the iron/alumina thermite. This may impact on the debris dispersion rates.

The initial conditions for the tests were assumed from an accident sequence initiated by a station blackout. The primary system and core melt conditions at the time of the HPME are associated with a pump seal LOCA followed by a instrument tube penetration failure. A mass of 55 grams of water was added to the cavity corresponding to a damp containment. The initial mass of melt (1.13 kg) was selected to match the total possible energy input of the simulant (0.713 kg) used in the IET tests. The energy sources include the thermal energy in the melt and also the energy resulting from chemical reactions. While the total overall energy content for the two materials is the same, a larger fraction of the energy comes from chemical reactions for the case of prototypic core material. Therefore, the energy input will be the same only if complete oxidation occurs.

RESULTS

Table 2 summarizes the initial conditions and results of three tests with corium, U1A, U1B and U2, along with the counterpart iron/alumina tests, IET-1RR and IET-6. The U1A, U1B and IET-1RR tests were conducted with a containment atmosphere initially inerted with nitrogen. This enables measurement of the hydrogen produced via melt/steam oxidation reactions. The U2 and IET-6 tests were specified with containment atmospheres that initially contained a nominal composition of one atmosphere air, one atmosphere nitrogen and a 2.6 mole% hydrogen. The hydrogen corresponds to 50% in-vessel oxidation of the zircaloy and subsequent release to the containment during the accident sequence.

The steam driving pressure in the tests varied from 3.0 MPa to 6.7 MPa. Figure 4 plots the accumulator blowdown histories obtained in each test.

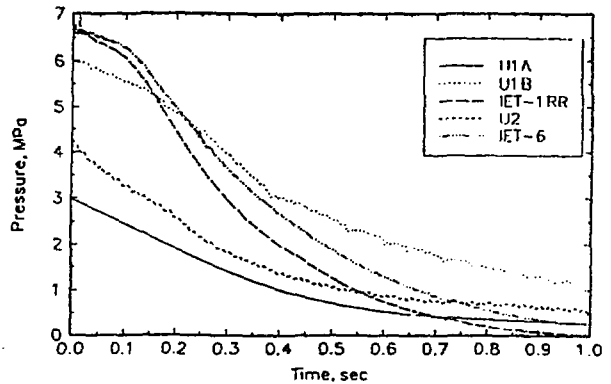


Figure 4 Blowdown Histories Obtained in the Experiments

Table 1 Oxidation Characteristics of Melt Simulants with Steam

Contributor	g-moles of H ₂ Produced per Mass Oxidized Fe/Al ₂ O ₃ w/Cr	g-moles of H ₂ Produced per Mass Oxidized Corium	Energy Released per Mass oxidized Fe/Al ₂ O ₃ w/Cr MJ/kg	Energy Released per Mass Oxidized Corium MJ/kg
Zr	0	3.00	0.0	0.88
Cr	3.11	1.07	0.45	0.16
Al	0.39	0.0	0.21	0.0
Total	3.50	4.07	0.66	1.04

The initial driving pressure is critical because it determines the time interval and rate of entrainment of melt from the cavity. The initial number of moles in the accumulator and injector is also critical because this may limit the extent to which the debris can be oxidized. The initial number of moles for each test is given in Table 2. In general the shapes of the curves for the corium tests were different. The iron/alumina test blowdown indicate an inflection point near 0.1 seconds that is not present in the corium test blowdown curves. The occurrence of this inflection point may be related to melt ejection process. The breach area was nominally the same for all the tests. However, the corium density is approximately a factor of two larger than the iron/alumina simulant density, which results in a smaller volume of melt to eject in the corium case.

Figure 5 gives a plot of the cavity and containment pressures for U1B.

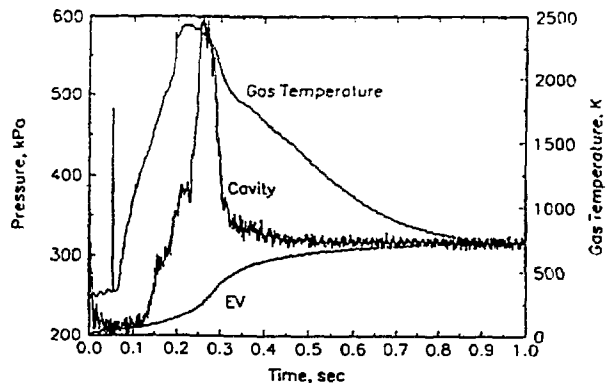


Figure 5 Cavity Pressure and Gas Temperature in DCH-U1B

Table 2 Summary of the Test Results

	U1A	U1B	IRR	U2	IET-6
Driving Pressure, P_0 , MPa	3.0	6.0	6.7	4.3	6.6
Blowdown Time, τ_b , sec	0.38	0.54	0.23	0.49	0.28
Blowdown Steam, N_b , g-moles	4.18	8.87	9.84	5.89	9.65
Initial Melt Mass, kg	1.130	1.130	0.820	1.130	0.713
Initial Cont. Pressure, P_{c0} , MPa	0.2	0.2	0.2	0.2	0.2
Initial Containment Atmosphere Composition, mole %					
H ₂	0.0	0.0	0.0	2.6	2.0
O ₂	0.12	0.57	0.47	11.6	9.9
N ₂	99.9	99.0	99.0	84.6	87.5
$\Delta P_{MAX, CAVITY}$, kPa	90	400	550	185	480
$\Delta P_{MAX, CONTAINMENT}$, kPa	45	111	150	185	250
$T_{MAX, CAVITY}$, K	740	2450	N/A	N/A	1600
Sweepout Fraction	0.190	0.795	0.705	0.295	0.691
H ₂ Pre-Existing, g-moles	0	0	0	3.1	2.3
H ₂ Produced, g-moles	5.0	6.0	4.1	6.0	4.9
O ₂ Depleted, g-moles	-0	-0	-0	3.0	2.1
H ₂ Burned, g-moles	0	0	0	6.0	4.2
Pressurization Efficiency	10.3	20.8	31.3	20.6	22.6

Similar data was obtained in all the tests. The interval over which a pressure difference between the cavity and containment exists corresponds to the time debris entrainment and sweepout from the cavity is occurring. The debris entrainment in the cavity is characterized by large heat transfer and oxidation rates. This entrainment process heats the blowdown gas to high temperatures as indicated by the cavity gas temperature plotted in Figure 5. The gas temperature was measured by an aspirated Type C thermocouple. A peak gas temperature of 2400 K was obtained in the U1B test compared to the 1500-1800 K range obtained in the IET tests. The measured peak gas temperature in U1A was 740 K. The cause of the lower gas temperature in U1A is the lower driving pressure leading to lower debris entrainment rates and less efficient mixing. This is indicated by the low debris fraction dispersed from the cavity. The debris dispersal was similar in U1B, IET-1RR and IET-6. The higher temperatures in the U1B corium compared to IET-1RR and IET-6 occurred due to the larger amount of chemical energy in the corium released during the cavity oxidation reactions. Large oxidation rates in the cavity during sweepout was indicated by gas samples. Gas sample measurements in the cavity during sweepout show droplet mole fractions in excess of 50 percent. However, more energy is transferred to the blowdown gas in the cavity in the U1B test than the iron/alumina simulant, due to the larger stored chemical energy in the corium compared to the iron/alumina simulant. The chemical energy content was discussed in detail in the previous section.

Figure 6 is a plot of the containment pressure histories obtained in the tests.

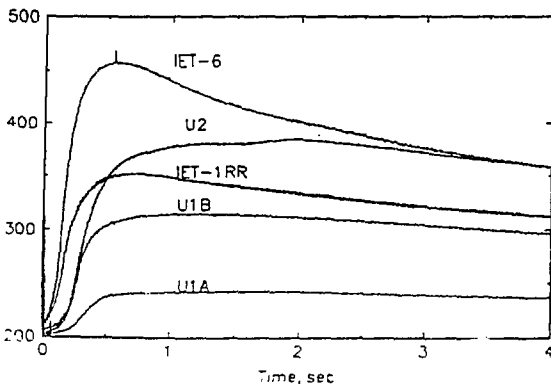


Figure 6 Containment Pressure Histories Obtained in the Experiment

Larger pressure increases obtained in the IET tests with alumina simulant is noted. A more meaningful way to compare the containment pressure histories for the tests is to dimensionalize the pressure and time with appropriate scaling variables. The containment pressure, P_c , is scaled by the maximum possible pressure increase, $\Delta P_{c,MAX}$, and initial pressure, $P_{c,0}$, to yield,

$$\Delta P_c^* = \frac{P_c - P_{c,0}}{\Delta P_{c,MAX}} \quad (1)$$

The maximum possible pressure rise is obtained from an adiabatic equilibrium calculation where all of the possible contributing energy sources to containment pressurization is considered. This same calculation was performed for the scaling analysis used to specify the initial mass of melt. Therefore, equation (1) defines a pressurization efficiency. Time is scaled with characteristic blowdown time of the primary system, τ_b , to yield,

$$t^* = \frac{t}{\tau_b} \quad (2)$$

Assuming choked flow a blowdown time is defined as,⁷

$$\tau_b = \frac{V_{RCS}}{C_d A_{BH} \sqrt{R_G T_0}} \quad (3)$$

where V_{RCS} is the primary system volume, C_d is a discharge coefficient, A_{BH} is the vessel breach hole area, R_G is the blowdown gas constant, and T_0 is the initial temperature of the blowdown gas. The blowdown times were obtained from the experimental data shown in Figure 4. Figure 7 is a plot of the containment pressure made dimensionless by the scaling indicated in equations (1) and (2).

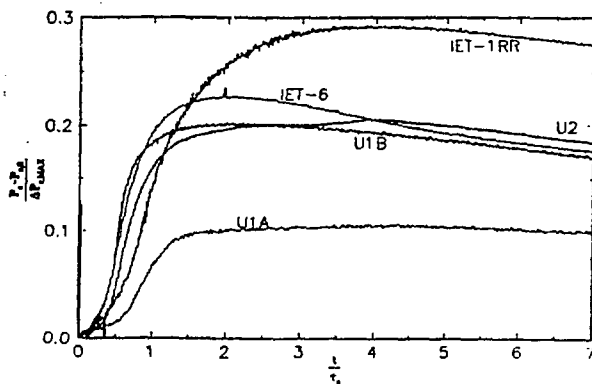


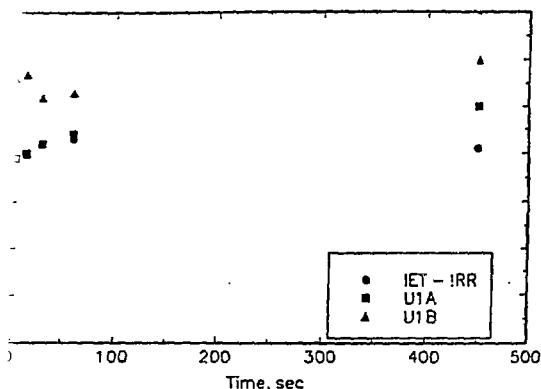
Figure 7 Containment Pressure History Plotted as an Efficiency

This plot reveals that the pressurization efficiency of the corium tests, U1A and U1B, were significantly lower than iron/alumina simulant test, IET-1RR, when the vessel was inerted. However, comparable efficiencies were obtained, for the tests that allowed hydrogen combustion.

The lower pressurization efficiency obtained in the inerted corium tests can be attributed in part to the lower driving pressures in these tests. A lower driving pressure leads to less efficient mixing of the debris, blowdown gasses and containment atmosphere. However, due to the large oxide fraction in the corium, freezing effects may also contribute to the lower efficiencies. Freezing effects will reduce the energy transfer because it will reduce debris entrainment, fragmentation and dispersal. In the non-inerted tests the pressurization efficiencies were much closer, despite the lower driving pressure in U2. The higher efficiency is due to the larger hydrogen production and combustion in the U2

mpared to IET-6. The details on the hydrogen tion and combustion results are given below. The results do not completely resolve the roles that pressure, larger hydrogen production and freezing played in determining the containment load. However, a clearly shows, these effects are important.

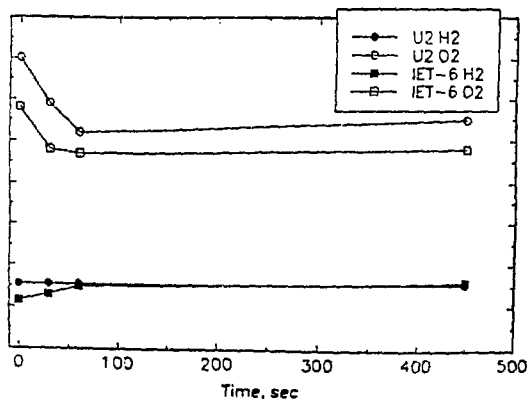
The gas sample analysis showed a significant increase rogen production for the corium compared to the rmina. Figure 8 is a plot of the number of g-moles of en in the containment at various times after the start HPME for the tests with an inert atmosphere.



8 Number of Hydrogen Moles in the Containment in the Inert Test

data indicate a larger hydrogen production for both orium tests, U1A and U1B, compared to the inert umina test, IET-1RR. This result was expected based discussion given above on the melt compositions. In s, the measured hydrogen production corresponds to te oxidation of the strong oxidizers (zirconium, um and aluminum) in the melt and oxidation of a fraction of the iron.

The analysis of the gas sample data is more cated for the non-inerted tests due to the combustion rogen. Figure 9 is a plot of the number of g-moles of and hydrogen in the containment at various times he start of the HPME for the U2 and IET-6 tests.



9 Number of Hydrogen and Oxygen Moles in the Containment in the Hydrogen Combustion Tests

The plot indicates the occurrence of the depletion of oxygen. The consumption of oxygen can occur for two reasons. The first is the combustion of hydrogen. The second is direct oxidation of the debris. The combustion of hydrogen is clearly evidenced by the larger pressurization that occurs compared to the inert atmosphere tests. The hydrogen combustion is also confirmed by video and high speed motion pictures taken during the experiment. These visualizations show a burning jet, as the blowdown gasses pass through the cavity, rise up through the subcompartment structures and into the upperdome.

With regard to hydrogen combustion the following phenomena appears to be occurring. The conversion of a significant fraction of the blowdown steam to hydrogen occurs during the cavity entrainment. These gasses are heated to temperatures in excess of 1000 K. The hot hydrogen and steam exit the cavity and rise up through the subcompartment to the upperdome. In the upperdome the jet accesses an oxygen containing atmosphere and the hydrogen is burned efficiently. Thus, a significant fraction, if not all of the oxygen is depleted by combining with hydrogen. However, some oxygen could be depleted due to direct debris oxidation. The amount is expected to be small for two reasons. First the blowdown of the primary system would displace a significant amount of the initial atmosphere out of the cavity and subcompartment into the upperdome. Secondly, a small amount of debris (0 - 10%) is dispersed to the upperdome. Therefore, it is considered a good bounding assumption to attribute all of the oxygen consumption to hydrogen combustion. This assumption yields a total of 6.0 g-moles and 4.2 g-moles of hydrogen consumed in U2 and IET-6, respectively.

A second point to note from the data in Figure 9 is the change in the amount of hydrogen moles in the test. For both tests the number of hydrogen moles remained approximately constant or slightly increased with respect to the initial condition in all of the samples. This indicates that hydrogen is burned as it is produced. From this data it can be inferred that a small fraction of the pre-existing hydrogen was burned in the tests. This inference is consistent with the jet burning phenomena observed and discussed above. In the case where the pre-existing hydrogen would burn it is expected that a flame would propagate throughout the upperdome. However, the burning jet appeared to be fueled by the gas exiting the cavity, where the preponderance of the hydrogen is produced. A flame propagating outward from jet the was not visible in the video or film. The results for the hydrogen combustion, obtained from the oxygen data, and the change in the hydrogen concentration is used to calculate the number of moles of hydrogen produced. A total of 6.0 g-moles and 4.9 g-moles of hydrogen are calculated to have been produced in U2 and IET-6, respectively. This data approximately agrees with the data obtained in the inert tests.

The final debris disposition was found to be sensitive to the initial driving pressure. In the IET-1RR, IET-6 and U1B tests the driving pressure varied from 6.0 to 6.7 MPa and the cavity sweep out fraction varied from 0.69 to 0.79. In the U1A and U2 tests the driving pressure was 3.0 and 4.3 MPa, respectively. The sweep out fraction for these tests was 0.19 and 0.30 for U1A and U2, respectively. The lower sweep out fractions are a result of the lower driving pressure producing lower cavity velocities and, consequently, lower

ainment rates. The fraction not trapped by the compartment and dispersed to the upper dome is also a matter of importance. This debris is expected to efficiently transfer the majority of its energy to the containment sphere. In the higher pressure tests a small but measurable amount of debris was dispersed to the upper dome. The dispersed upper dome fraction varied from 0 to 0.12 in these tests. In the lower pressure tests no measurable amount of debris was dispersed to the upper dome. The driving pressure in UIB (6.0 MPa) was lower than in IET-1RR (6.7 MPa) and IET-6 (6.6 MPa) and debris dispersal was higher in UIB. This is contrary to existing data which indicates debris dispersal increasing with increasing driving pressure and decreasing melt density.⁸ A possible reason for this result may have been the longer down time, τ_d , in UIB which resulted in a longer time to drain particles. However, due to the scarcity of data on debris dispersal over a wide range of pressures, no firm conclusions can be drawn on the effect of melt simulant on debris dispersal.

SUMMARY

Direct containment heating integral experiments using non-prototypic core materials have been conducted. These experiments complement the IET tests that were conducted at Sandia National Laboratory and Sandia National Laboratories. The IET experiments used iron/alumina simulant with chromium as a core melt simulant. The objective of the experiments reported on here was to explore debris dispersal distortions, introduced by a non-prototypic core melt, in IET tests. The results of the tests indicated important differences between the iron/alumina simulant and prototypic materials. These differences are discussed.

A comparison of the thermophysical properties of the actual corium and the iron/alumina simulant was made.

The iron/alumina simulant is found to have larger available energy content. However, if completely oxidized by the corium will liberate a larger amount of chemical energy. This results because a significant fraction of the metal phase is zirconium, whereas, the iron/alumina phase is predominantly iron. Due to this difference, the iron/alumina will potentially produce more hydrogen from steam reactions. The corium contains a larger oxide fraction, with a correspondingly higher freezing range. Corium has approximately a factor of two larger density. The experiments were conducted in the 1/40 scale Sandia National Power Plant geometry used in the IET tests. A small corium mass was selected by the energy to volume ratio used for the IET tests. The total possible energy input was the same for the corium and iron/alumina simulant tests; however, the distribution between chemical and thermal energy is different.

Two corium experiments were conducted with an inert atmosphere, UIA and UIB. The measured peak pressure load and the pressurization efficiency was lower in the corium tests compared to the counterpart iron/alumina simulant tests. The hydrogen production was 20% to 30% lower in the corium tests. A third corium test, U2, was conducted with an atmosphere that contained approximately 1 mole% oxygen and 2.6 mole% hydrogen. This test

produced a lower peak pressure than the counterpart iron/alumina test, IET-6. However, the pressurization efficiencies are similar for the two non-inerted tests. The U2 test gas sample data indicated that more hydrogen was produced and burned than in IET-6. In the IET tests and UIB the driving pressure was greater than 6.0 MPa and the debris dispersal was similar. For these tests 70% to 80% of the debris was swept out of the cavity and 6% to 12% of that debris was dispersed to the upperdome. In the tests with lower driving pressure, UIA and U2, a significantly larger fraction of the debris was retained in the cavity and no debris was dispersed to the upperdome. This data suggests that the debris dispersal is very sensitive to the driving pressure. No firm conclusion can be made on the effect of debris simulant on dispersal due to the small available data set.

The DCH integral test data reported on here demonstrate that important differences exist between iron/alumina thermite core melt simulant and actual prototypic materials. These differences must be accounted for when using the results of the IET experiments to assess the actual power plant response. The experiments showed that lower driving pressures and corium freezing effects produced lower pressurization efficiencies. The hydrogen production was larger in the corium tests due to the higher fraction of reactive metals in the melt. However, the tests showed, as in the IET tests, that produced and pre-existing hydrogen is not sufficiently burned on a time scale with the DCH event to produce a containment threatening pressure response. Additional future work is focusing on the theoretical modeling of the DCH phenomena to help bring about issue closure.

ACKNOWLEDGEMENTS

Richard Wesel provided technical assistance on the experiments. Dennis Kilsdonk prepared figures of the facility.

The work was supported by U. S. Nuclear Regulatory Commission under FIN No. A22669.

REFERENCES

1. Binder, J. L., L. M. McUmbler and B. W. Spencer, "Quick Look Data Report on the Integral Effects Test 1RR in the COREXIT Facility at Argonne National Laboratory," ANL/RE/LWR92-3, May 1992a.
2. Binder, J. L., L. M. McUmbler and B. W. Spencer, "Quick Look Data Report on the Integral Effects Test 3 in the COREXIT Facility at Argonne National Laboratory," ANL/RE/LWR92-7, July 1992b.
3. Binder, J. L., L. M. McUmbler and B. W. Spencer, "Quick Look Data Report on the Integral Effects Test 6 in the COREXIT Facility at Argonne National Laboratory," ANL/RE/LWR92-8, August 1992c.
4. Allen, M. D., M. Pilch, R. O. Griffith and D. C. Williams and R. T. Nichols, "The Third Integral Effects Test (IET-3) in the Surtsey Test Facility," SAND92-0166, March 1992a.

Allen, M. D., M. Pilch, R. O. Griffith, R. T. Nichols and T. K. Blanchat, "Experiments to Investigate the Effects of 1:10 Scale Zion Structures on Direct Containment Heating (DCH) in the Surtsey Test Facility: The IET-1 and IET-1R Tests," SAND92-0255, July 1992b.

Allen, M. D., T. K. Blanchat, M. Pilch and R. T. Nichols, "An Integral Effects Test in a Zion-Like Geometry to Investigate the Effects of Pre-Existing Hydrogen on Direct Containment Heating in the Surtsey Test Facility: The IET-6 Experiment," SAND92-1802, January, 1993

Zuber, N., B. Boyack, A. Dukler, P. Griffith, J. Healzer, R. Henry, M. Ishii, J. Lehner, S. Levy, F. Moody, M. Pilch, B. Sehgal, B. Spencer, T. Theofanous, J. Valente, G. Wilson and W. Wulff, "An Integrated Structure and Scaling Methodology for Severe Accident Technical Issue Resolution," NUREG/CR-5809, EGG-2659, 1991.

Tutu, N. K., et al. "Debris Dispersal from Reactor Cavities During High Pressure Melt Ejection Accident Scenarios," NUREG/CR-5146, BNL-NUREG-52147, July 1988.